

On the Stability of the 421-day Periodicity in A0538–66

K.E. McGowan^{1,2*}, P.A. Charles^{2,3}

¹*Los Alamos National Laboratory, Los Alamos, NM 87545, USA*

²*Department of Physics, University of Oxford, Oxford OX1 3RH*

³*Department of Physics & Astronomy, University of Southampton, Southampton, SO17 1BJ*

Accepted Received

ABSTRACT

In this paper we analyse 70 years of archival Harvard and Schmidt plate data of the 16.6 d Be X-ray binary A0538–66 in order to search for the presence of the long-term period of 420.82 ± 0.79 d found in MACHO photometry (Alcock et al. 2001). We find evidence for a long-term period of 421.29 ± 0.95 d in the archival data, and examine its stability. We also combine the archival and MACHO datasets in order to improve the accuracy of the orbital period determination, using a cycle-counting analysis to refine its value to 16.6460 ± 0.0004 d. We also test the model proposed in our previous paper (Alcock et al. 2001) with observations documented in the literature for A0538–66 from 1980–1995, constraining the system inclination to be $i > 74.9 \pm 6.5^\circ$.

Key words: binaries: close - stars: individual: A0538–66 - X-rays: stars

1 INTRODUCTION

A0538–66 is a recurrent X-ray transient in the LMC (White & Carpenter 1978), which contains a neutron star (X-ray pulsations were detected by the Einstein Observatory; Skinner et al. 1982) orbiting a bright ($B \sim 15$) Be star. At various times the source exhibits He II $\lambda 4686$ emission and P Cygni profiles have been detected on Balmer and He I lines (e.g. Charles et al. 1983). These spectral features with such high velocity components are not seen in classical Be stars. The system was found to have an orbital period of 16.6515 ± 0.0005 d from the recurrence of its outbursts (Skinner 1981; hereafter S81), which are interpreted as arising in a highly eccentric orbit (Charles et al. 1983).

In a previous paper (Alcock et al. 2001; hereafter Paper I) we analysed ~ 5 years of optical monitoring of A0538–66 by the MACHO project. This revealed a remarkably stable long-term modulation of 420.82 ± 0.79 d, together with the previously known 16.6510 ± 0.0022 d period, hitherto interpreted as being orbital in origin. A model was presented in Paper I in which the origin of the long-term period is due to the formation and depletion of an equatorial disc surrounding the Be star. In this model, as the disc forms, the material shrouds the Be star and the brightness of the source is reduced, as is observed in the light curve (see Fig. 8, top panel; which is based on Fig. 1 of Paper I). The neutron star is then able to accrete from the circumstellar matter and outbursts can occur. The successive neutron star passages deplete the available material and the source is seen to brighten. Once all the material is accreted, or ejected, the

source returns to a quiescent state in which the naked Be star can be observed.

To investigate the periodicities found in Paper I we have analysed archival photometric data of A0538–66 from S81. To test our model we have compared the times of predicted outbursts with observations of A0538–66 from the literature.

2 ARCHIVAL PHOTOGRAPHIC DATA

In 1981 Skinner analysed archival UK Schmidt and Harvard photographic B -band plates of A0538–66, taken between 1915 and 1981. From these observations he derived the 16.6515 d orbital period, and an ephemeris of $T_0 = \text{MJD } 2443423.96$, which has been the basis for studies of A0538–66 over the last 20 years. Our MACHO observations revealed the presence of the same orbital modulation with a period of 16.6510 d (see Paper I), which within errors confirms Skinner’s orbital period for A0538–66. It was noted that the outbursts observed in the MACHO light curve are much smaller than those found by S81 and Densham et al. (1983). Our aim in analysing the archival plate data was to investigate both the presence and stability of this long-term period over the much longer interval (~ 70 years) of the archival plate material. Skinner’s data is plotted in Fig. 1.

2.1 The 421 d cycle

To search for the long period found from the MACHO photometry we first removed the 16.65 d periodic outburst events from the archival plate data. Using our *a priori* knowledge, we searched for a periodicity near to 420.82 d.

* email: mcgowan@lanl.gov

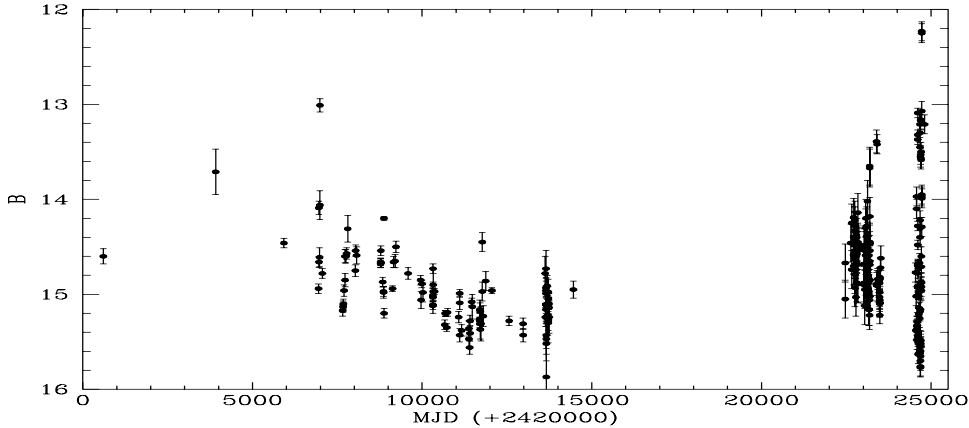


Figure 1. Archival plate data (S81) showing the light curve of A0538-66 from April 1915 to July 1981.

We performed the temporal analysis using a phase dispersion minimisation (PDM) periodogram (Stellingwerf 1978) over the frequency range 2.32×10^{-3} – 2.44×10^{-3} cycle d^{-1} , with a resolution of 1.5×10^{-7} cycle d^{-1} (Fig. 2). The lowest peak in the PDM corresponds to $P = 421.29$ d, which is within the error for the MACHO period. We propagated an error for the peak in the PDM periodogram by a Monte Carlo simulation in which we created artificial light curves with the same mean and standard deviation as the archival light curve. We calculated PDMs for each artificial dataset. We then employed a centroiding technique in which the mode of the peaks near the peak of interest that are below a user defined threshold is calculated. We find $P = 421.29 \pm 0.95$ d, which again encompasses the MACHO period. To assess the significance of this period, we performed a period search over a longer frequency range, namely 0.001 – 0.01 cycle d^{-1} , with a resolution of 1×10^{-6} cycle d^{-1} (Fig. 3). We employed a PDM periodogram and Lomb-Scargle (LS) periodogram (Lomb 1976; Scargle 1982) for the temporal analysis.

The results from the longer search indicates that the 421.29 d period is significant. However, the LS periodogram has many peaks above the 99% confidence level. We created two simulated light curves using a Gaussian random number generator with the same mean and standard deviation as the archival data. One contained an added sinusoidal signal with a frequency equal to that of the highest peak in the LS periodogram, while the other contained a signal corresponding to 421.29 d. We then constructed a LS periodogram for each simulated light curve, with the same frequency range and resolution as for the longer search. The peaks present in the LS periodogram for the simulated light curves (Fig. 3, third and fourth panels) show that the LS periodogram structure in the real data cannot distinguish between the presence of one or two periods. It is also possible that the periodogram can be due to one frequency which shifts slightly over the time span of the dataset. The latter case is more likely given the nature of the long-term periods in Be systems. Hence we find marginal evidence, given the poorer quality of the plate data, for a comparable periodicity to that found in the MACHO data.

We folded the archival data on $P = 421.29$ d, using the

MACHO ephemeris $T_0 = \text{JD } 2449002.109$ (see Paper I), and then binned the data, to investigate the form of the modulation (Fig. 4). The folded and phase binned light curves indicate that there is a periodic modulation present. The form of the variability is marginally different to that for the MACHO data, as the flat section of the folded light curve we obtained for the MACHO data is not evident (see Fig. 8, top panel). However, this may be due to there being a much greater uncertainty in the B magnitudes determined from the archival plates which leads to a larger scatter in the archival light curve. We also note that a far greater number of cycles are used to create the folded light curve of the archival data. We find that the modulation in the MACHO light curve varies from cycle to cycle, this may also be occurring in the archival data, however the scatter would mask this.

2.2 The 16.6 d orbital period

We also investigated whether we could determine an improved orbital period and ephemeris for our combined dataset spanning 83 years, comprising the archival plate data and the MACHO data. S81 found an orbital period of 16.6515 ± 0.0005 d for the archival data and we found $P = 16.6510 \pm 0.0022$ d for the MACHO data. Before we could search for a common period we had to detrend the archival data; as for the MACHO data, this was achieved by subtracting a third order polynomial from the dataset. We then combined these data with the detrended MACHO data (see Paper I).

Due to the highly non-sinusoidal nature of the outburst modulation seen in both the archival data (see Fig. 7) and the MACHO data (Fig. 8), a Fourier-based period search is not appropriate. A PDM was performed for a frequency range 0.055 – 0.065 cycle d^{-1} with a resolution of 8.25×10^{-7} cycle d^{-1} , the resulting periodogram shows substantial fine structure which makes determining the true period difficult (Fig. 5). The minimum value in the PDM found using the centroiding technique, with an error propagated with a Monte Carlo simulation as before, is $P = 16.6466 \pm 0.0002$ d. The value for the period found from the combined archival plate data and the MACHO data is lower than the periods

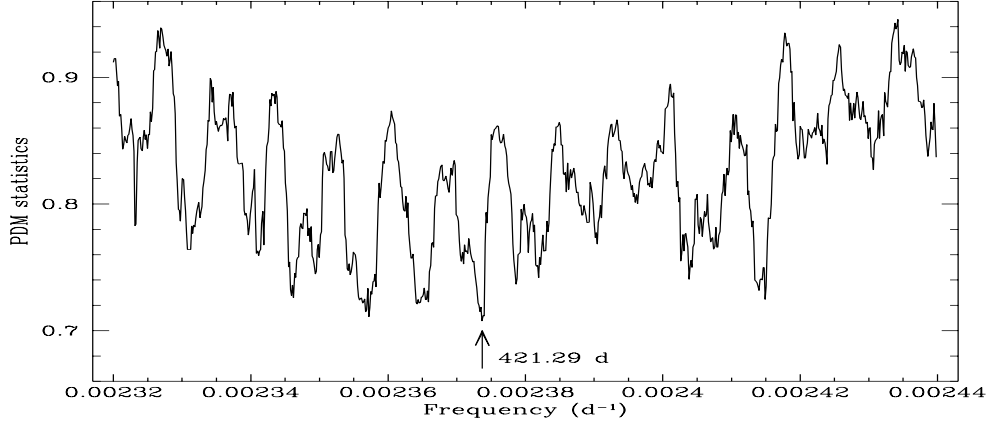


Figure 2. Phase dispersion minimisation periodogram for the archival data. A frequency range of 2.32×10^{-3} – 2.44×10^{-3} cycle d^{-1} was searched with a resolution of 1.5×10^{-7} cycle d^{-1} .

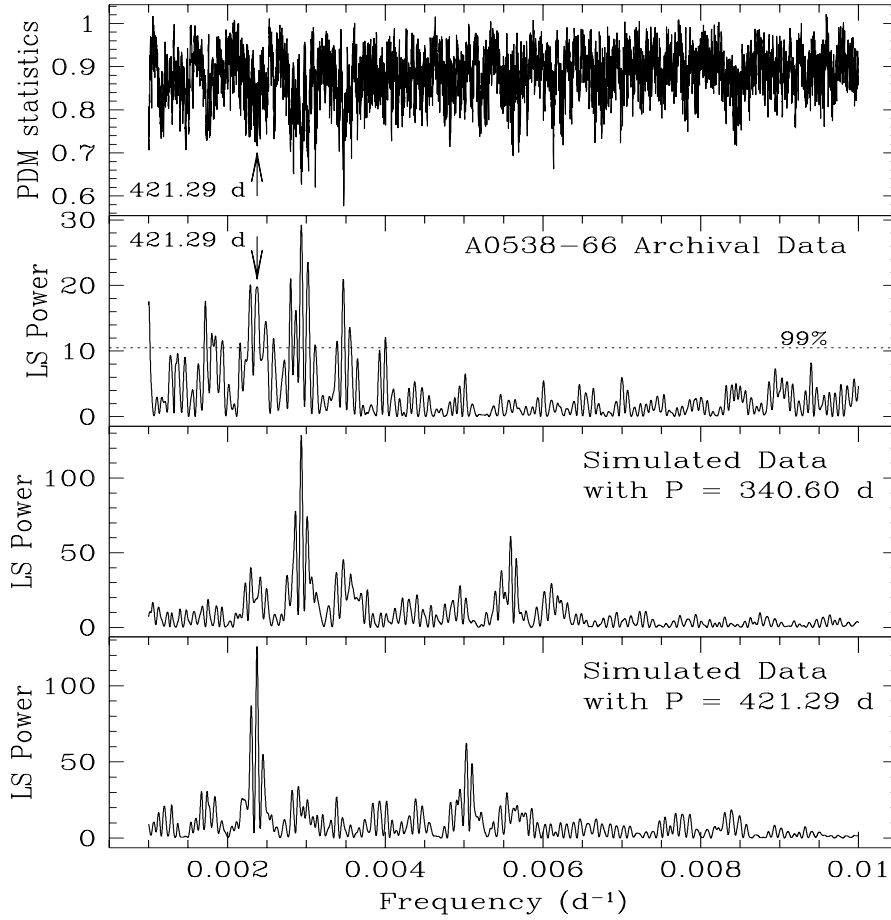


Figure 3. Phase dispersion minimisation (first panel) and Lomb-Scargle periodograms (second panel) for the archival data over a frequency range of 0.001 – 0.01 cycle d^{-1} , with a resolution of 1×10^{-6} cycle d^{-1} . The third and fourth panels show the Lomb-Scargle periodograms for the simulated light curves, which contained a sinusoidal signal of 340.60 d and 421.29 d, respectively.

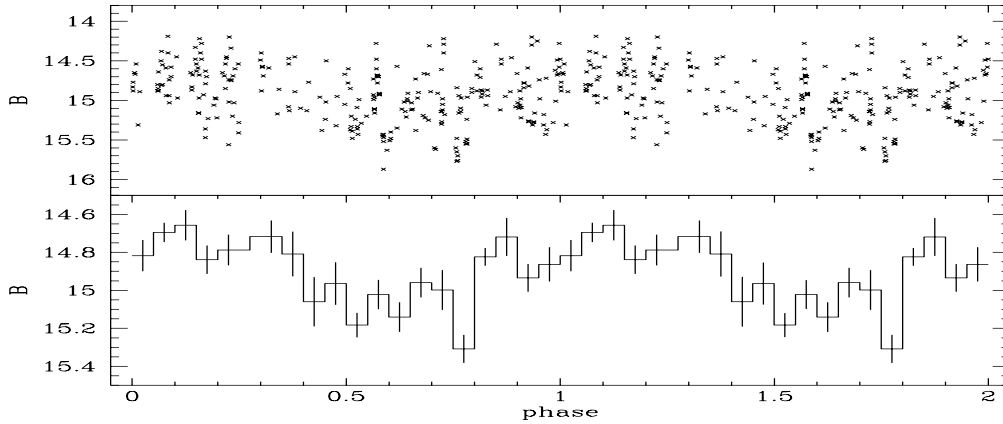


Figure 4. Archival data folded on $P = 421.29$ d with $T_o = \text{JD } 2449002.109$ (top), and in 20 phase bins (bottom). Error bars for the binned light curve are the standard errors on the mean for the data points in each bin.

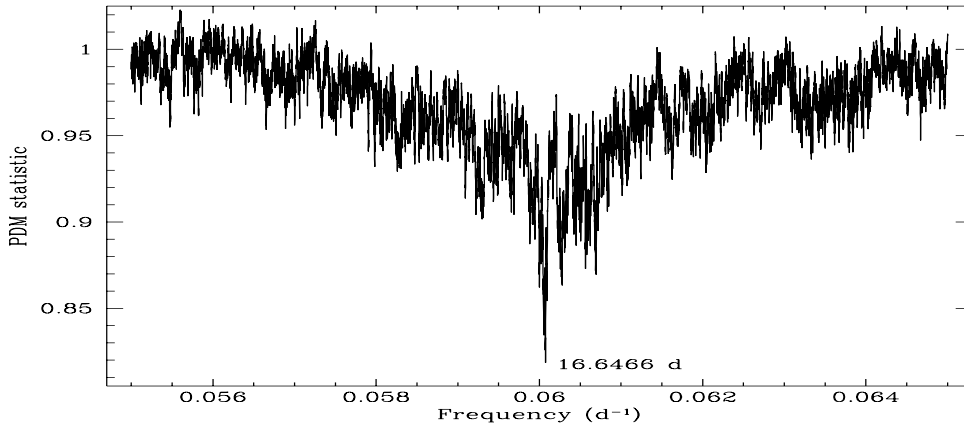


Figure 5. Phase dispersion minimisation for the combined archival and MACHO data. Frequency range $0.055\text{--}0.065$ cycle d^{-1} with resolution 8.25×10^{-7} cycle d^{-1} .

found for each dataset alone (see S81 and Paper I, respectively). The error found also does not encompass the previous values. We note that the range of periods investigated in the combined search is narrower and the resolution finer than the previous searches.

To refine this result we attempted a cycle-counting analysis of the outburst timings. We divided the combined data into 6 sections. We then took the period given by S81 and folded and phase-binned each section of data on it, using an arbitrary phase zero (T_o). The phase of the peak of the outburst (ϕ_{outburst}) was estimated with an error determined from the other points in the peak. The time for the outburst peak is given by $T_{\text{outburst},n} = T_{o,n} + \phi_{\text{outburst}} \times P_{\text{outburst}}$, where $T'_{o,n} = T_o + \text{int}[(T_{\text{midpt}} - T_o)/P_{\text{outburst}}] \times P_{\text{outburst}}$, in order to give a time close to the mid-point time (T_{midpt}) of the n th dataset. We are left with a set of 6 ephemerides spanning over 83 years, which should all agree with a single recurrence period. For each cycle and trial period, a time of minimum is predicted (C) which is then compared to the observed time (O), and a simple χ^2 minimisation for the $O-C$ values versus the trial period then gives a best-fit period of

16.6460 ± 0.0004 d, and ephemeris $T_o = \text{MJD } 2441443.1432$ (Fig. 6). The $O-C$ plot for the best-fit period is shown in Fig. 6.

The combined data were folded and phase-binned on the best-fit period and ephemeris derived from the cycle counting method (Fig. 7). The value for the best-fit period is again lower than the period found in S81 and Paper I.

3 ARCHIVAL DATA FROM 1980–1995

By studying previous observations of A0538–66 from the literature we are able to investigate our proposed model for the 421 d cycle. A0538–66 is known to exhibit recurrent optical and X-ray outbursts on its orbital period. By convention the source is described as being “active” when such outbursts occur (which coincide with when the source is optically bright). The “quiescent” phase is taken to be when no outbursts are detected, coinciding with when the source is optically faint. Many observations of A0538–66 have been taken near phase zero of the 16.6 d period hoping to detect outbursts, some have been successful, while others not.

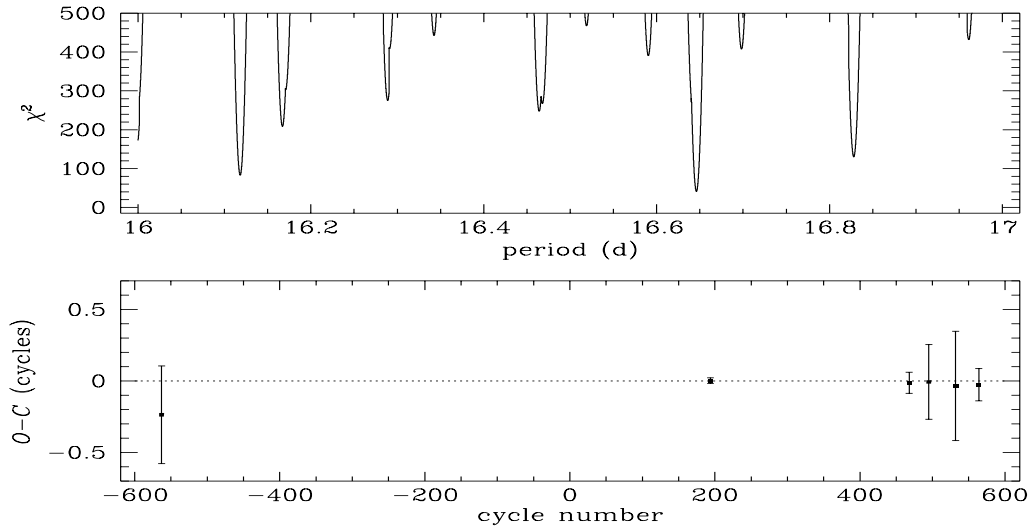


Figure 6. χ^2 for the predicted versus observed times of outburst maximum, for a corresponding range of periods (top panel). Within the range of possible periods consistent with the PDM result, there is one minimum from the cycle counting approach which has a smaller χ^2 than any others. Bottom panel, for the best fit period of 16.6460 d, the observed (O) – computed (C) times of outburst maximum (for sections in which the outburst peak was present in both the folded and bin-folded data at a significant level only) are shown, in terms of cycles.

In our model A0538–66 is only in an active state, and hence outbursts can occur, during the extended dip phase in the 421 d cycle, when the system is faint. The brightness of the source decreases due to the formation of the Be star’s equatorial disc, as the neutron star passes through this disc it accretes material leading to outbursts. Successive orbits of the neutron star depletes the circumstellar matter causing the brightness of the source to increase. A0538–66 then returns to quiescence when accretion, or ejection, of all the disc material has occurred. While the source is in quiescence it is seen to be optically bright as we observe only the naked B star. With our model we can predict times when the source should display outbursts, and when the bare B star can be observed.

It is clear then that the previously used *active/quiescent* terminology is too crude to cover the range of behaviour that is observed. Therefore, using our model we have defined the following activity states for the source :

- **ACTIVE** : in the 421 d cycle the source is only active during the extended dip, i.e. $\phi_{421} = 0.36\text{--}0.94$
- **high** : in the active state, times of optical/X-ray outburst, or mini-outburst, predicted by the 16.6 d orbital period, i.e. $\phi_{16} = 0.96\text{--}0.2$
- **low** : times when outbursts should not be seen in the active state
- **QUIESCENT** : times when only the naked B star should be seen in the 421 d cycle, i.e. $\phi_{421} = 0.94\text{--}0.36$

Fig. 8 (top panel) shows the MACHO V -band light curve folded on the 421 d period, the dashed lines indicate the lower and upper limits for the active phase. There is uncertainty in the lower limit for the active phase in the 421 d cycle due to the ill-defined ingress into the dip, which can be as low as $\phi_{421} = 0.13$. The dotted line demonstrates the low-

est limit that could be considered as an active phase for the 421 d cycle. The bottom panel of Fig. 8 shows the detrended V -band light curve of A0538–66 folded on the best-fit 16.6 d period, the dashed lines indicate the high state phase interval.

To see if our model agrees with observations we have taken published data of A0538–66 from 1980–1995 and calculated the phases of each observation on the 421 d cycle. We have also calculated the phases for the observations using the newly determined best-fit period and ephemeris, $P = 16.6460$ d and $T_0 = \text{MJD } 2441443.1432$, respectively. A summary of the active and quiescent observations and how they relate to our model is given below. Details of the archival observations and their phases, calculated with reference to our model, are shown in Table 1 which is only available electronically via http://www.raptor.lanl.gov/NoFrame_Publications.htm.

3.1 Active

3.1.1 High State

Optical spectra of A0538–66 taken during the active high state show a number of features. In general, the spectra are dominated by Balmer and He I emission with P Cygni profiles (Charles et al. 1983; Corbet et al. 1985; Corbet et al. 1997; Misselt, Clayton & Shulte-Ladbeck 1998). The emission lines indicate the presence of a disc. At times of outburst maximum He II $\lambda 4686$, which is characteristic of X-ray binaries, is observed (Charles et al. 1983; Hutchings et al. 1985; Corbet et al. 1985; Menzies, Feast & Howarth 1983). The presence of He II $\lambda 4686$ emission just prior to outburst maximum (i.e. $\phi_{16} \gtrsim 0.96$) and post outburst maximum ($\phi_{16} \gtrsim 0.1$) is varied. Corbet et al. (1985) do not detect He II emission in pre-outburst maximum spectra taken in 1983 which agrees

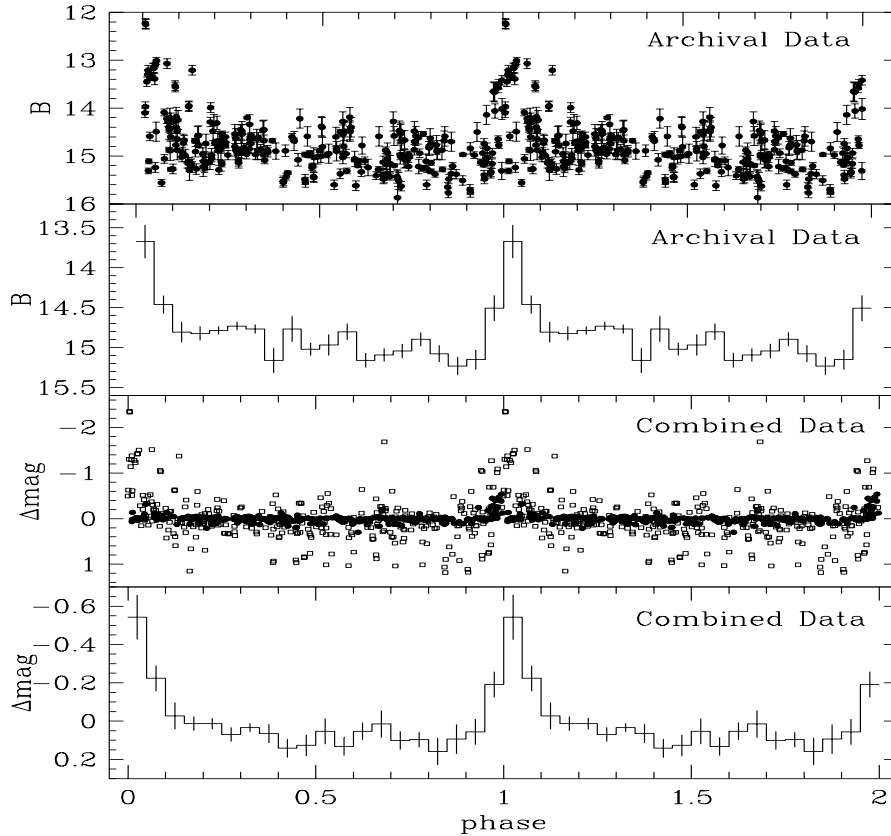


Figure 7. Archival plate data (S81) folded on $P = 16.6515$ d using $T_0 = \text{MJD } 2443423.96$ (first panel), and in 20 phase bins (second panel). Combined MACHO and archival A0538–66 data folded on the best-fit period of 16.6460 d with $T_0 = \text{MJD } 2441443.143$, archival data are plotted as open squares, MACHO data are plotted as filled circles (third panel), and in 20 phase bins (fourth panel). Error bars for the binned light curve are the standard errors for the data points in each bin.

with observations of Charles et al. (1983), however Corbet et al. (1985) found He II emission in observations from 1982. The spectra from 1983 also exhibit H and He I absorption, while H β is in emission (Corbet et al. 1985). He II is not found in spectra taken after outburst maximum by Corbet et al. (1997) and Misselt et al. (1998), but Charles et al. (1983) do detect it.

Howarth et al. (1984) described their UV spectra as “outburst”, “inter-outburst” and “quiescent”. The distinction between “outburst” and “inter-outburst” was made based on the shape and strength of the continuum, and the strength of the C IV $\lambda 1550$ emission. The UV spectra taken during the active high state classed as “outburst” spectra show strong, broad C IV $\lambda 1550$, N V $\lambda 1240$ and He II $\lambda 1640$ emission. The “outburst” spectra all have $0.0 < \phi_{16} < 0.1$. The two high state spectra classed as “inter-outburst” taken before outburst maximum show C IV $\lambda 1550$ and N V $\lambda 1240$, but no He II $\lambda 1640$ emission. The emission features in the UV spectra obtained by Charles et al. (1983) that coincided with an optical outburst ($B = 12.7\text{--}12.81$) agree with the “outburst” spectra taken by Howarth et al. (1984).

ROSAT observations by Campana (1997) were described as quiescent due to the low flux observed. However, we find that the highest X-ray luminosity measured

of $1 \times 10^{36} \text{ erg s}^{-1}$ occurs during an active high state. We suggest that this simply corresponds to a low-amplitude outburst. This is similar to the Corbet et al. (1997) observations which they attribute to an outburst of low-amplitude. Their active high state *ASCA* observation measured an average X-ray luminosity of $\sim 5.5 \times 10^{36} \text{ erg s}^{-1}$.

3.1.2 Low State

Active low state optical spectra display an early-type absorption spectrum. Emission lines of H, He I and He II $\lambda 4686$ are also detected (Murdin, Branduardi-Raymont & Parmar 1981; Charles et al. 1983; Corbet et al. 1985). In addition to Balmer and He I absorption, Smale et al. (1984) find weak H β and H γ emission. The lines display inverted P Cygni profiles which vary, they suggest this is due to the infall of material. The presence of a disc is again inferred from the Balmer emission.

The UV active low state spectra of A0538–66 show no He II $\lambda 1640$ emission, but C IV $\lambda 1550$ and N V $\lambda 1240$ emission are present (Howarth et al. 1984). The lines can also display P Cygni profiles (Charles et al. 1983).

ROSAT observations by Campana (1997) show that the

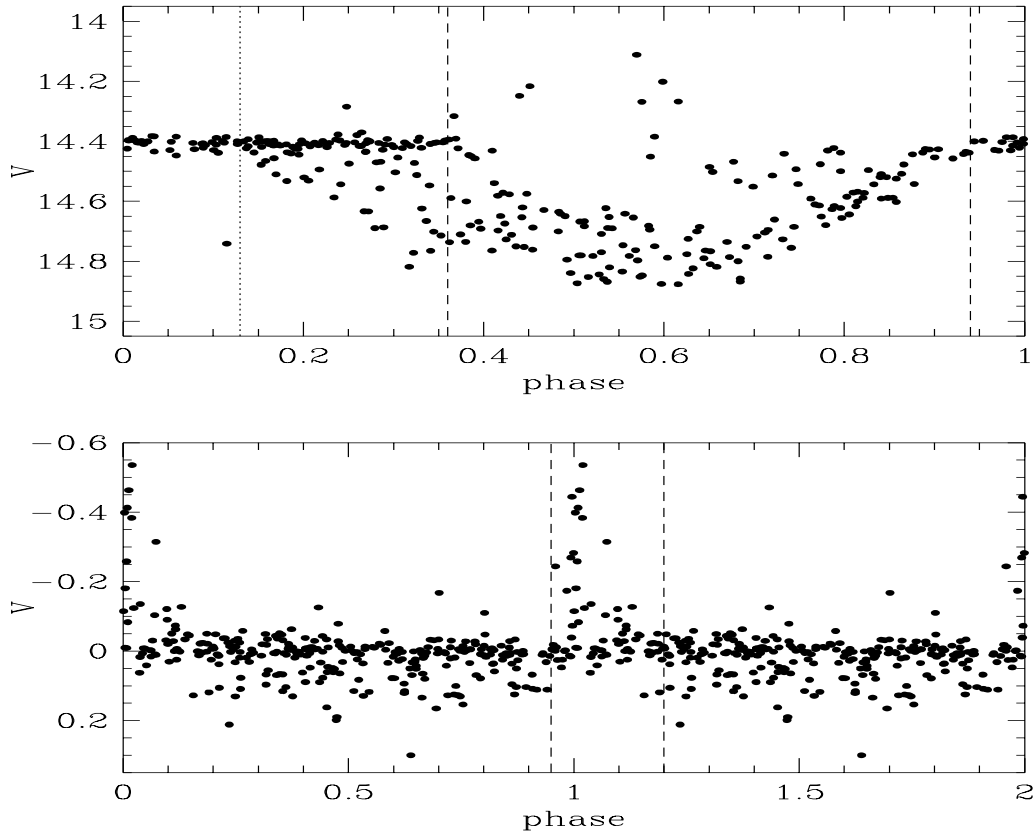


Figure 8. The MACHO *V*-band light curve folded on $P = 420.82$ d with $T_0 = \text{JD } 2449002.109$ (top panel), and the detrended light curve folded on $P = 16.6460$ d with $T_0 = \text{MJD } 2441443.1432$ (bottom panel). The dashed lines indicate the phases of activity for the 421 d cycle (top panel) and the high state for the 16.6 d period (bottom panel), the ranges are $\phi_{421} = 0.36\text{--}0.94$ and $\phi_{16} = 0.96\text{--}0.2$, respectively. The dotted line in the top panel indicates the uncertainty for the lower limit for the activity phase in the 421 d cycle, and corresponds to $\phi = 0.13$.

X-ray luminosity of A0538–66 varies from $3 \times 10^{34} \text{ erg s}^{-1}$ to $1 \times 10^{35} \text{ erg s}^{-1}$ during the active low state.

3.2 Quiescent

Quiescent optical spectra are characterised by Balmer and He I absorption (Smale et al. 1984; Hutchings et al. 1985; Misselt et al. 1998). Hutchings et al. (1985) do not detect any Balmer emission characteristic of a disc, however Smale et al. (1984) find evidence for weak $\text{H}\beta$ and $\text{H}\gamma$ emission. One observation of Misselt et al. (1998) shows only an absorption spectrum, while the other shows an absorption spectrum with $\text{H}\beta$ and $\text{He II } \lambda 4686$ emission. In our model an absorption spectrum only should be observed during quiescence as we are viewing the naked Be star. The presence of emission lines can possibly be explained by the uncertainty in the beginning of the ingress into the extended dip, which can move the start of the active phase to $\phi_{421} = 0.13$. Howarth et al. (1984) find very weak or no $\text{C IV } \lambda 1550$ emission in their quiescent UV spectra. Measurements of the X-ray luminosity of A0538–66 in quiescence yield values $\lesssim 1 \times 10^{35} \text{ erg s}^{-1}$.

3.3 Photometry

We find that a wide range of magnitudes are measured for A0538–66 during both active high and low states, and during quiescence. The outbursts recorded by Corbet et al. (1985) and van Paradijs et al. (1984), all but one outburst observed by Charles et al. (1983) and one outburst from Densham et al. (1984) fall in our active high state. The rest of the photometric observations occur during the active low state, or quiescence. The original classification of the active and quiescent phases relied on the brightness of the source. Our model finds that the source is in its extended “active” phase when the source is faint, hence we cannot be certain of the state due to the magnitude alone. Generally, the lowest magnitudes observed for A0538–66 are found to coincide with our active low state which agrees with our model predictions.

We note that Densham et al. (1983) recorded the brightest outbursts of A0538–66 at the end of 1981 and the beginning of 1982. We find that only one of these observations is during an active high state using our model. In general however, our model seems to agree with the previously published observations. It seems that our model can fit outbursts of

normal intensity, but is unable to fit the unusually bright ones observed by Densham et al. (1983).

4 SYSTEM INCLINATION

If we assume that the fading and brightening events in A0538–66’s MACHO light curve are due to the formation and depletion of the equatorial disc around the Be star, we can make a simple estimate of a lower limit for the inclination of the system.

Using the quoted range of spectral type (Charles et al. 1983) and temperature (Allen 1973) for the Be star in A0538–66 we can determine an average effective temperature for the star. Assuming a blackbody spectrum at $\lambda = 550$ nm (\sim Johnston *V*), and using the effective temperature above, we can calculate the intensity that would be observed from a normal B star. By taking the observed difference between the ‘flat’ part and the dip minimum from the MACHO *V*-band light curve (Fig. 8) we can determine the intensity that would be observed at the minimum. By comparing the intensity calculated for a normal B star alone and the intensity for the B star and disc, we can calculate the percentage loss in intensity due to the disc at its maximum extent, assuming our model is correct.

The Be star and disc can then be represented simply by a half circle (for the unobscured hemisphere) and half an ellipse (for the obscured hemisphere). The semi-minor axis of the ellipse is related to the inclination angle for the system, $b = R \cos i$, where b is the semi-minor axis of the ellipse, R is the radius of the star, and i is the inclination.

This assumes that the disc covers all of the star on the obscured hemisphere at radii greater than the semi-minor axis, and that the disc is not emitting any light. This therefore sets a lower limit for i , since if the disc were contributing to the observed magnitude, the inclination would have to be higher to cover more of the star to compensate for the light from the disc. We find that the lower limit for the inclination of A0538–66 is $74.9 \pm 6.5^\circ$.

5 CONCLUSIONS

The orbital period for A0538–66 was determined by S81 using archival plates. We re-analysed these data to investigate the stability of the long-term period found in the MACHO data. Given our *a priori* knowledge, we find evidence for periodic variability on $P = 421.29 \pm 0.95$ d for the archival data, which agrees with the MACHO period ($P = 420.82 \pm 0.79$ d), within errors. This indicates that the ~ 420 d cycle persists over a much longer interval than presented in Paper I. However, long-term monitoring of the source must continue in order to answer this question convincingly.

We also refined the orbital period and ephemeris by combining the MACHO and plate data. A straight-forward period search of the combined data using a PDM periodogram led to a period of 16.6466 ± 0.0002 d. This period is lower than those found by S81 ($P = 16.6515 \pm 0.0005$ d) and from the MACHO data ($P = 16.6510 \pm 0.0022$ d). We performed a cycle-counting analysis to refine the period and found $P = 16.6460 \pm 0.0004$ d, with an ephemeris of $T_0 = \text{MJD } 2441443.143$. The period found is shifted by 0.0055 d

from that of S81 using the archival plate data alone, and by 0.0050 d from the period for the MACHO data.

We have studied published archival data from 1980–1995 to test our model for A0538–66. Our results show that our model is in general consistent with the observations. However, the published observations largely correspond to our inactive states for the source. A real test of our model is to observe an outburst, or mini-outburst, at a time predicted by our model.

By assuming that our model is correct i.e. the long-term modulation is due to the formation and depletion of the Be star’s equatorial disc, and using the observed drop in intensity in the MACHO *V*-band light curve, we can determine a lower limit for the inclination of the system of $i = 74.9 \pm 6.5^\circ$.

6 ACKNOWLEDGEMENTS

We thank Gerry Skinner for providing a copy of the archival Schmidt and Harvard data.

REFERENCES

- Alcock C., et al., 2001, MNRAS, 321, 678 (Paper I)
- Campana S., 1997, A&A, 320, 840
- Charles P.A., et al., 1983, MNRAS, 202, 657
- Corbet R.H.D., Mason K.O., Córdova F.A., Branduardi-Raymont G., Parmar A.N., 1985, MNRAS, 212, 565
- Corbet R.H.D., Charles P.A., Southwell K.A., Smale A.P., 1997, ApJ, 476, 833
- Densham R.H., Charles P.A., Menzies J.W., van der Klis M., van Paradijs J., 1983, MNRAS, 205, 1117
- Howarth I.D., Prinja R.K., Roche P.F., Willis A.J., 1984, MNRAS, 207, 287
- Hutchings J.B., Crampton C., Cowley A.P., Olszewski E., Thompson I.B., Suntzeff N., 1985, PASP, 97, 418
- Lomb N.R., 1976, Astrophys. Space Sci., 39, 447
- Menzies J., Feast M., Howarth I., 1983, IAU Circ., 3858
- Misselt K.A., Clayton G.C., Schulte-Ladbeck R.E., 1998, PASP, 110, 396
- Murdin P., Branduardi-Raymont G., Parmar A.N., 1981, MNRAS, 196, 95
- Scargle J.D., 1982, ApJ, 263, 835
- Skinner G.K., 1981, Space Sci. Rev., 30, 441 (S81)
- Skinner G.K., Bedford D. K., Elsner R. F., Leahy D., Weisskopf M. C., Grindlay, J., 1982, Nature, 297, 568
- Smale A.P., Charles P.A., Densham R.H., Bath G.T., van Paradijs J., Menzies J.W., Skinner G.K., 1984, MNRAS, 210, 855
- Stellingwerf R.F., 1978, ApJ, 224, 953
- van Paradijs J., van Amerongen S., de Kool M., Pakull M., Deul E.R., Lub J., Greve A., 1984, MNRAS, 210, 863
- White N.E., Carpenter G.F., 1978, MNRAS, 183, 11